Acta Phys. Hung. B 26/1–2 (2006) 173–180
DOI: 10.1556/APH.26.2006.1–2.20

QUANTUM
ELECTRONICS

State Space Geometry of a Double-Loop Interferometer

Stefan Filipp,[1,@] Yuji Hasegawa,[1] Rudolf Loidl[1,2] and Helmut Rauch[1]

[1] Atominstitut der Österreichischen Universitäten, 1020 Wien, Austria

[2] Institut Laue Langevin, 38042 Grenoble, France

[@] Corresponding author; E-mail: sfilipp@ati.ac.at

Received 3 August 2006

Abstract. The phase of a quantum state comprises information about the geometry of the state space. For example, in a magnetic field the spin state of a neutron traces out a particular path in its spherical shaped state space and the geometric phase acquired during this evolution reflects the curvature of this sphere. But the geometric phase is not only restricted to the spinor wave function, also the path of the neutron in an interferometer gives rise to a non trivial momentum state space and consequently to a geometric phase. Experimental results for a non-cyclic evolution are presented that are in agreement with theoretical predictions derived purely from geometrical considerations. By obeying a parallel transport condition dynamical contributions could largely be avoided and the measured phase is of geometric nature.

Keywords: neutron optics, geometric phase, dephasing
PACS: 03.65.Vf, 03.75.Dg, 61.12.Ld, 05.40.-a, 02.60.-x

1. Introduction

Already in the 50's Pancharatnam [1] investigated the phase change of light when changing its polarization by use of filters. This change in phase is based on the spherical shape of the polarization state space. A seminal paper by Berry [2] in 1984 was finally the catalyst for a vast number of investigations in the geometry of state space. He demonstrated that the adiabatic and cyclic transport of a quantum mechanical system involves a phase contribution to the final state that is neither dependent on the evolution time nor on the energies involved. A canonical example is a spin-1/2 particle in a slowly changing magnetic field. The spin follows the adiabatic changes of the field and accumulates a phase in a cyclic evolution that consists of a dynamical and a geometric part. Simon [3] immediately noticed the

1589-9535/ $ 20.00

connection to differential geometry and the representation of the geometric phase in terms of a fiber bundle along with a particular connection given by the adiabaticity condition. Soon after there have been several extensions in various directions, e.g. to degenerate Hamiltonian systems [4], to non-adiabatic [5] and non-cyclic evolutions [6] and to an off-diagonal geometric phase [7]. A purely kinematic description has been formulated by Mukunda and Simon [8]. Also for mixed states a geometric phase can be defined [9–11].

Besides these theoretical work numerous experiments have been performed to verify geometric phases using various types of quantum mechanical systems, e.g. polarized photons [12] or NMR [13]. The spin-1/2 property of neutrons is particularly suited for explicit demonstrations of geometric phenomena [14–17].

The geometric phase originates from the transport of a state vector in Hilbert space. It is independent of the particular physical property that is represented by the Hilbert space, be it a particle's spin or its (angular) momentum. In interferometry the which-way freedom of the incident particle is also connected to a two-dimensional Hilbert space in the same manner as the spinor representation. In general, Feynman et al. [18] stated that the description of any two-level quantum system is equivalent to the description of a spin-1/2 particle. Exploiting this equivalence there is in principle no difference between manipulations in the spin space of neutrons with the orthogonal basis $\{|\uparrow\rangle, |\downarrow\rangle\}$ as eigenstates of σ_z, and in momentum space with $\{|k\rangle, |k'\rangle\}$ as orthogonal basis vectors corresponding to two directions of the neutron beam in an interferometer. An even more appropriate description for the interferometric case for the forthcoming discussion is in terms of "which-way" basis states $\{|p\rangle, |p^{\perp}\rangle\}$, namely, if the neutron is found in the upper beam path after a beam-splitting plate it is said to be in the state $|p\rangle$, or in the state $|p^{\perp}\rangle$, if found in the lower beam path.

Some of the authors studied already the cyclic spatial geometric phase experimentally [15], however, their results admit some ambiguities in the interpretation. The experiment has therefore been criticized by Wagh [20] later. He concludes that in this setup the phase picked up by a state during its evolution is merely a U(1) phase factor stemming from the dynamics of the system and not due to the geometric nature of the subjacent Hilbert space. In [19] the present authors have presented first results on the extension of the previous setup to non-cyclic evolutions, dismissing thereby excoriated points. Further details are shown in the following in order to substantiate the geometric interpretation of the measured results.

2. Theoretical Considerations

A double-loop interferometer as depicted in Fig. 1 (left) has been used in order to measure the geometric phase obtained by the state evolution of $|\psi_t^0\rangle$ in the second loop relative to the reference beam $|\psi_r^0\rangle$. While the state $|\psi_t^0\rangle$ is split once more at the beam-splitter BS3 and is manipulated by an absorber (A) and a phase shifter (PS2), on the reference beam only an additional phase shift is imposed. The final

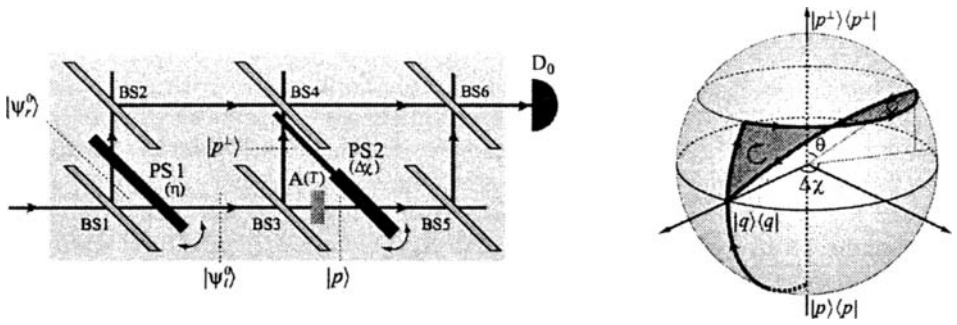

Fig. 1. Experimental setup utilizing a double-loop perfect-crystal neutron interferometer. One loop is used for the state manipulation with a phase shifter (PS2) together with a beam attenuator (A) and the other one provides a reference beam with adjustable phase by use of the phase shifter (PS1)

state of the former is denoted by $|\psi_f\rangle$. By a rotation of the first phase shifter (PS1) about an angle η interference fringes are recorded which disclose the relative phase difference $\Phi \equiv \arg\langle\psi_r|\psi_f\rangle$ between $|\psi_f\rangle$ and $|\psi_r\rangle$. By a suitable choice of attenuator A and phase shifter PS2, Φ is equal to the geometric phase accumulated by $|\psi_t\rangle$ during its traversal of the second loop. Changing the transmission coefficient T and the phase shifts χ_1 and χ_2 in the second loop alters the path of $|\psi_t\rangle$ in its state space and consequently also the geometric phase.

To justify the geometric nature of the measured phase the path on the Bloch sphere representing the state space can be devised. The solid angle enclosed by the path shown in Fig. 1 (right) is proportional to the geometric phase and these purely geometrical considerations constitute a check whether the claims to measure a geometric phase are valid. The solid angle can be calculated numerically and results in the same curves as one finds by calculating the intensity pattern of the superposed neutron beams in the double-loop interferometer.

Indeed, the interference pattern of the intensity measured by varying η is determined by

$$|e^{i\eta}|\psi_r\rangle + |\psi_f\rangle| \propto I_r + I_t + 2|\langle\psi_r|\psi_f\rangle| \cos(\eta - \arg\langle\psi_r|\psi_f\rangle) \tag{1}$$

with $I_r = \langle\psi_r|\psi_r\rangle$ and $I_f = \langle\psi_f|\psi_f\rangle$ is shifted by $\arg\langle\psi_r|\psi_f\rangle$. Explicitly,

$$\Phi \equiv \arg\langle\psi_r|\psi_f\rangle = \frac{\chi_1 + \chi_2}{2} - \arctan\left[\tan\left(\frac{\Delta\chi}{2}\right)\frac{1-\sqrt{T}}{1+\sqrt{T}}\right], \tag{2}$$

and by carefully tuning the transmission T and the phase shifts Φ is exactly the geometric phase of the state evolution.

What is the condition that the measured value is determined only by the path on the sphere? According to Mukunda and Simon [8] the geometric phase is defined

by

$$\phi_g = \arg\langle\psi_r|\psi_f\rangle - \phi_d\,, \tag{3}$$

i.e. the total phase minus the dynamical phase ϕ_d. For a special choice of the phase shifting slabs in PS2 dynamical phase contributions ϕ_d are made to vanish so that $\phi_g = \Phi = \arg\langle\psi_r|\psi_f\rangle$. More precisely, in order to avoid any dynamical terms the state has to be *parallel transported*, that is, the scalar product $\langle\psi_t(\xi)|\psi_t(\xi+\delta)\rangle$ between two neighboring states has to be real. In our case the state transport is accomplished by imposing the phase shift $\chi_1(\xi) = -Cd_1\xi$ on the reflected and $\chi_2(\xi) = Cd_2\xi$ on the transmitted beam at BS3, where ξ denotes the rotation angle and d_1 and d_2 the thickness of the phase shifter slab in the beam $|p^\perp\rangle$ and $|p\rangle$, respectively. $C = N_{Al}b_c\lambda$ with N_{Al} the particle density and b_c the coherent scattering length of aluminum. $\lambda = 2.715$ Å is the mean wavelength of the incident neutrons. The state in the second interferometer loop is given by

$$|\psi(\xi)\rangle \propto (\sqrt{T_1}e^{i\chi_1(\xi)}|p^\perp\rangle + \sqrt{T_2}e^{i\chi_2(\xi)}|p\rangle)\,, \tag{4}$$

where we take also the intrinsic absorption along the path $|p^\perp\rangle$ into account by introducing the transmission coefficient T_1. The scalar product between two infinitesimally close states is

$$\langle\psi(\xi)|\psi(\xi+\delta\xi)\rangle = (T_1e^{-iCd_1\delta\xi} + T_2e^{iCd_2\delta\xi})\,. \tag{5}$$

The imaginary part vanishes, if $-T_1\sin(Cd_1\delta\xi) + T_2\sin(Cd_2\delta\xi) = 0$ or

$$T_1d_1 = T_2d_2 \tag{6}$$

for small δ. This provides the parallel transport condition which guarantees vanishing dynamical phase.

If the parallel transport condition is not fulfilled the integral of all the infinitesimal contributions divided by the norm of the state defines the dynamical phase [8],

$$\phi_d \equiv \int_{-\xi/2}^{\xi/2} \frac{C(-d_1T_1 + T_2d_2)s}{\langle\psi(s)|\psi(s)\rangle}ds = \sqrt{2}N_{Al}b_{cAl}\lambda\frac{(d_2T_2 - d_1T_1)\xi}{T_1+T_2} = \frac{T_1\chi_1 + T_2\chi_2}{T_1+T_2}\,. \tag{7}$$

3. Experimental Results

In Fig. 2 the results for different ratios $d_1/d_2 = T_2/T_1$ are shown. The solid line indicates the fit to the measured phase shift Φ and the theoretical predictions are represented by the dotted line. The latter also comprises a linear term originating from additional dynamical phase contributions, for example, due to a not perfectly parallel phase shifter PS2.

The obtained data mirrors the geometric nature of the measured phase. Especially, we notice the increase of the phase up to $\Delta\chi = \pi/2$ corresponding to an

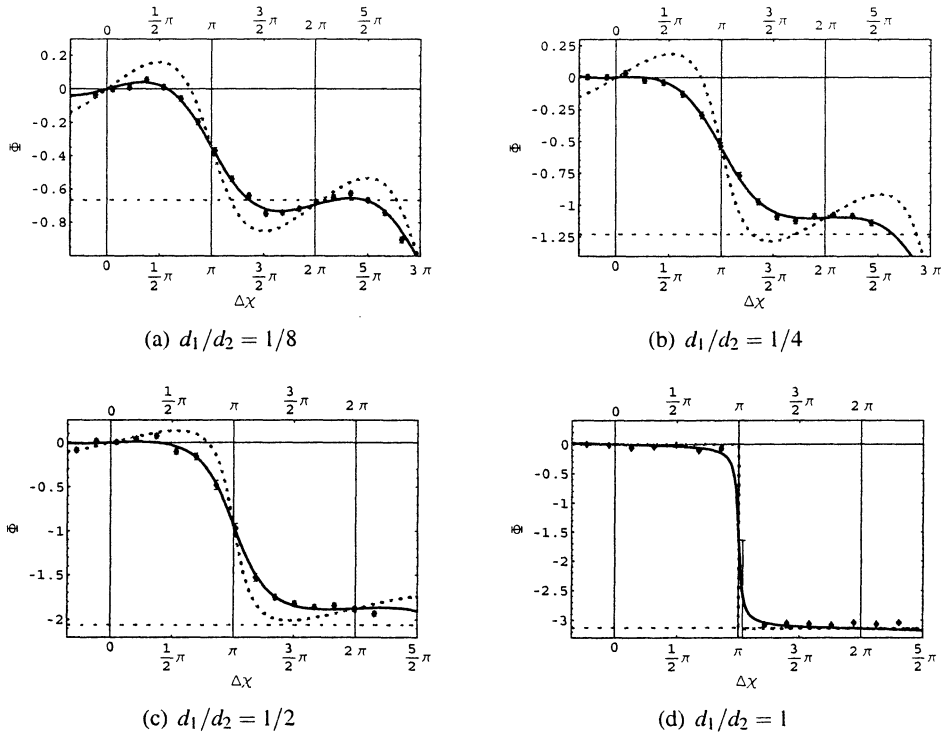

(a) $d_1/d_2 = 1/8$ (b) $d_1/d_2 = 1/4$

(c) $d_1/d_2 = 1/2$ (d) $d_1/d_2 = 1$

Fig. 2. Observed phase shift Φ for a non-cyclic evolution of the state vector parameterized by the relative phase shift $\Delta\chi$. The dotted line indicates the theoretical prediction for the geometric phase assuming hundred percent visibility, whereas the solid line takes the diminished visibility into account. The dotted straight line is the measured geometric phase for $\Delta\chi = 2\pi$ when remaining dynamical contributions are subtracted

increase of the enclosed solid angle. From this point on there is a decrease since the second part of surface area on the Bloch sphere is compassed in the opposite direction causing an additional minus sign for the solid angle (cf. Fig. 1 (left)). In the $(d_1/d_2 = 1)$-setup a phase jump of π is observed pertinent to the transport of the state along the equatorial line with no surface enclosed up to $\Delta\chi = \pi$. For $\Delta\chi > \pi$, $\Omega = 2\pi$ and therefore the geometric phase $\Phi = \Omega/2 = \pi$.

The straight line indicate the measured geometric phase for a cyclic evolution with $\Delta\chi = 2\pi$. This value has been corrected for the dynamical contribution and coincides with the measured curve at $\Delta\chi = 2\pi$ in the $(d_1/d_2 = 1)$- and $(d_1/d_2 = 1/8)$-setup since in these measurements there is almost no dynamical phase involved. In the other cases small dynamical contributions lead to an observable difference between the expected geometric and the measured phase.

3.1. Discussion on the additional phase shifts

The qualitative agreement with the theoretically expected value is quite good for all these setups, however, one notices two different modifications. First, there is a flattening of the curves and second there is a compression along the ordinate. Hence, to fit the data Eq. (2) is inapt as it stands, but

$$\mathcal{F}(\xi; C, D) = \frac{\chi_1(\xi) + \chi_2(\xi)}{2} - \arctan\left[\tan\left(\frac{\Delta\chi(\xi)}{2}\right)\frac{\sqrt{T_1} - C\sqrt{T_2}}{\sqrt{T_1} + C\sqrt{T_2}}\right] + D\xi \quad (8)$$

has to be used instead. C is responsible for the flattening and D is an extra linear term that takes additional dynamical contributions leading to the compression into account. The latter term is mainly due to a slight mismatch in the adjustment of the ratio $d_1T_1 = d_2T_2$ as demanded by the parallel transport condition (6) as well as a deviation in the initial position of PS2. If the angle between the forward beam direction and the surface of the plates is not exactly 45° the effective thicknesses change and the parallel transport condition is not fulfilled completely.

What is the physics behind the additional phase shift represented by the fit coefficient C? On the one hand side the neutron beam is neither perfectly monochromatic nor collimated, hence, a plane wave approximation is not fully valid. Instead, a particular momentum distribution is attributed to the coherent neutron wave-packet. This wave-packet structure comprises the coherence properties [21]. The beam is only coherent up to a certain coherence order and consequently unequal phase shifts in the beam paths lead to a loss of coherence. From another point of view, the wave-packet is spatially displaced by a beam splitter and if finally the partial beams do not overlap anymore, the visibility vanishes. For large displacements so-called Schrödinger cat states are formed [22]. In our experiment phase shifting plates of unequal thickness are placed into the different beam paths and consequently unequal phase shifts of many orders difference are imposed on the different beam paths. This causes the flattening of the experimental curve.

In particular, the intensity comprises contributions from the superposition of three beams, each with a different phase factor and an attenuation factor,

$$\begin{aligned} I &= |e^{i\eta} + \sqrt{T_1}e^{i\chi_1} + \sqrt{T_2}e^{i\chi_2}|^2 \quad (9)\\ &= 1 + T_1 + T_2 + 2\sqrt{T_1T_2}\cos\Delta\chi + 2\sqrt{T_1}\cos(\eta - \chi_1) + 2\sqrt{T_2}\cos(\eta - \chi_2)\,. \end{aligned}$$

The three cosine terms denote the interference oscillations between each beam pair. Varying η causes a sinusoidal interference pattern. Indeed the two η-dependent cosine terms can be subsumed into one and we find,

$$I = 1 + T_1 + T_2 + 2\sqrt{T_1T_2}\cos\Delta\chi + 2\left[\sqrt{T_1^2 + T_2^2 + 2T_1T_2\cos\Delta\chi}\cos(\eta - \Phi)\right]$$

with Φ given by

$$\Phi = \frac{\chi_1 + \chi_2}{2} - \arctan\left[\tan\left(\frac{\Delta\chi}{2}\right)\frac{\sqrt{T_1} - \sqrt{T_2}}{\sqrt{T_1} + \sqrt{T_2}}\right], \quad (10)$$

i.e. the shift of the interference pattern is determined by the transmission coefficients T_1 and T_2 as in Eq. (2).

Now, for the reasons discussed above the cosine terms in Eq. (9) are exponentially damped due to the different spatial displacement in the different beams and the intensity reads,

$$I' = 1+T_1+T_2+2\sqrt{T_1}e^{-\Gamma_1}\cos(\eta-\chi_1)+2\sqrt{T_2}e^{-\Gamma_1}\cos(\eta-\chi_2)+2\sqrt{T_1T_2}e^{-\Gamma_{12}}\cos\Delta\chi\,. \tag{11}$$

Although all the discussion about the parallel transport remains valid, because the state transport itself is still the same, it becomes evident that there appears an additional phase shift due to the Γ factors. The new Φ' is different from Φ in Eq. (10) whenever $e^{-\Gamma_1} \neq e^{-\Gamma_2}$:

$$\Phi' = \frac{\chi_1+\chi_2}{2} - \arctan\left[\tan\left(\frac{\Delta\chi}{2}\right)\frac{\sqrt{T_1}-(e^{-\Gamma_2}/e^{-\Gamma_1})\sqrt{T_2}}{\sqrt{T_1}+(e^{-\Gamma_2}/e^{-\Gamma_1})\sqrt{T_2}}\right]. \tag{12}$$

In other words, only if the displacements are same in both $|p\rangle$ and $|p^{\perp}\rangle$ relative to the reference beam $|\psi_r^0\rangle$ there is no influence from the finite coherence length. But, since we have phase shifting slabs of different thicknesses and therefore different Γ_1 and Γ_2, an additional phase shift is natural. This effect is more pronounced for neutrons of lower incident energy.

4. Conclusions

We have extended the discussion on the spatial geometric phase in a double-loop interferometer to non-cyclic evolutions. Different paths accompanied by different geometric phases have been implemented to investigate the state-space geometry of the underlying two-dimensional Hilbert space spanned by the path eigenstates. We have identified dynamical contributions and provided a parallel transport condition which has to be fulfilled in order to avoid them. A proper choice of transmission coefficients and phase shifts in the second-loop gives a purely geometric phase, hence information about the state space geometry. In all settings systematic deviations from the theoretical curve are observed. These effects have been explained on the basis of the finite coherence length of the neutron beam. The exponential damping factors of the visibility between the individual partial waves lead to an observable additional phase shift. This does not affect the geometric nature of the measured phase, since the state evolution is not affected and still fulfills the parallel transport condition.

Acknowledgments

This research has been supported by the Austrian Science Foundation (FWF), Project Nr. F1513.

References

1. S. Pancharatnam, *Proc. Ind. Acad. Sci.* **A44** (1956) 247.
2. M.V. Berry, *Proc. R. Soc. Lond. A* **392** (1984) 45.
3. B. Simon, *Phys. Rev. Lett.* **51** (1983) 2167.
4. F. Wilczek and A. Zee, *Phys. Rev. Lett.* **52** (1984) 2111.
5. Y. Aharonov and J.S. Anandan, *Phys. Rev. Lett* **58** (1987) 1593.
6. J. Samuel and R. Bhandari, *Phys. Rev. Lett.* **60** (1988) 2339.
7. N. Manini and F. Pistolesi, *Phys. Rev. Lett.* **85** (2000) 3067.
8. N. Mukunda and R. Simon, *Ann. Phys.* **228** (1993) 205.
9. A. Uhlmann, *Rep. Math. Phys.* **24** (1986) 229.
10. E. Sjöqvist et al., *Phys. Rev. Lett.* **85** (2000) 2845.
11. S. Filipp and E. Sjöqvist, *Phys. Rev. Lett.* **90** (2003) 050403; *Phys. Rev. A* **68** (2003) 042112.
12. A. Tomita and R. Chiao, *Phys. Rev. Lett.* **57** (1986) 937.
13. J. Du et al., *Phys. Rev. Lett.* **91** (2003) 100403.
14. T. Bitter and D. Dubbers, *Phys. Rev. Lett.* **59** (1987) 251.
15. Y. Hasegawa et al., *Phys. Rev. A* **53** (1996) 2486.
16. Y. Hasegawa et al., *Phys. Rev. Lett.* **87** (2001) 070401; *Phys. Rev. A* **65** (2002) 052111.
17. J. Klepp et al., *Phys. Lett. A* **342** (2005) 48.
18. R.P. Feynman, F.L. Vernon and R.W. Hellwarth, *J. Appl. Phys.* **29** (1957) 49.
19. S. Filipp et al., *Phys. Rev. A* **72** (2005) 021602(R); *NIST J. Res.* **110** (2005) 251.
20. A.G. Wagh, *Phys. Rev. A* **59** (1999) 1715.
21. H. Rauch et al., *Phys. Rev. A* **53** (1996) 902.
22. M. Baron and H. Rauch and M. Suda, *J. Opt. B* **5** (2003) 8241.